CONF-950846--73

UCRL-JC-121636 Rev 1
PREPRINT

High Energy-Density Physics: From Nuclear Testing to the Superlasers

E. M. Campbell, N. Holmes, S. B. Libby,
B. A. Remington, and E. Teller

This paper was prepared for submittal to the
1995 APS Topical Conference on
Shock Compression of Condensed Matter
Seattle, WA
August 13-18, 1995

October 20, 1995

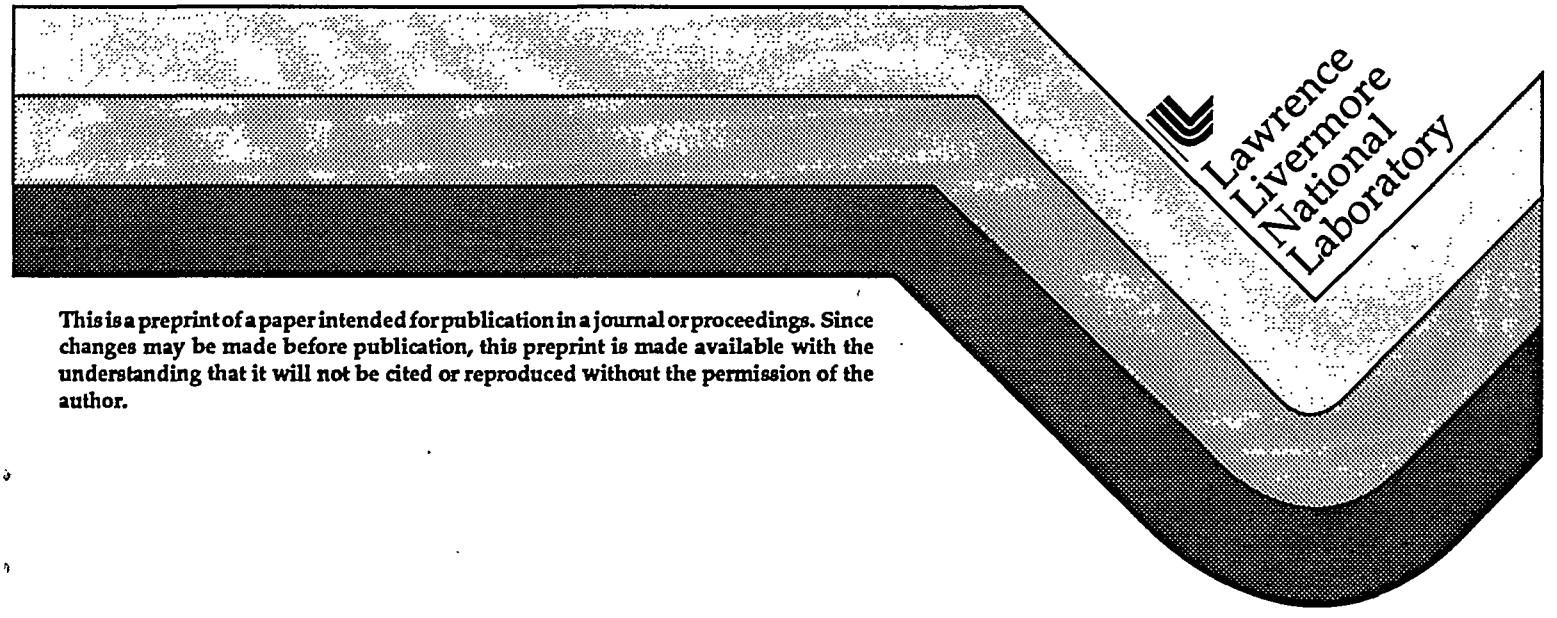

HIGH ENERGY-DENSITY PHYSICS: FROM NUCLEAR TESTING TO THE SUPERLASERS

E. M. Campbell, N. C. Holmes, S. B. Libby, B. A. Remington, and E. Teller

Lawrence Livermore National Laboratory, Livermore, CA 94550

We describe the role for the next-generation "superlasers" in the study of matter under extremely high energy density conditions, in comparison to previous uses of nuclear explosives for this purpose. As examples, we focus on three important areas of physics that have unresolved issues which must be addressed by experiment: equations of state, hydrodynamic mixing, and the transport of radiation. We will describe the advantages the large lasers will have in a comprehensive experimental program.

INTRODUCTION

In the event of a comprehensive nuclear test ban treaty, mankind would lose access to a regime of high energy-density physics that has been difficult to attain by other known means. This has led to a proposal from Chelyabinsk, Russia to resume nuclear testing, but purely for scientific research purposes.(1) However, with the advent of the proposed next-generation "superlasers" such as the U.S. National Ignition Facility (NIF),(2) and the French Laser Megajoule Project (LMJ),(3) the capability to focus 1-2 megajoules of energy into sub-millimeter-scale volumes at power levels of 500 TW will become routine. These lasers are being built to spearhead the international effort in controlled nuclear fusion through inertial confinement (4,5) (ICF) and, indeed, to open new regimes for high energy density physics research.(6) With the advent of megajoule class lasers, one recovers the ability to access very high energy-density regimes hitherto extant only at the cores of stars and in nuclear detonations. The question to be briefly explored in this paper is exactly what are some of the regimes that the superlasers can access that were previously achievable only in a nuclear experiment. In a brief discourse, this topic obviously cannot be treated in a comprehensive fashion. Instead, we will mention only three areas as examples: equation of state, hydrodynamic mixing, and radiation physics. These topics are representative of areas that have already been studied at Nova class lasers.(6) A wide range of other possible topics, suchs as plasma physics with 10^7–10^8 gauss local magnetic fields, or experiments with the intense (10^{18}) neutron burst expected from the NIF capsule ignition will not be addressed here. We will close with a brief discussion of some of the advantages of the superlasers.

EQUATION OF STATE

One of the main goals in high energy-density physics is to understand the behavior of matter at high pressure and density. (7) Areas of physics where this is relevant include basic condensed matter physics, planetary physics, geophysics, astrophysics, and ICF. Other high-energy density research problems, such as radiation transport and hydrodynamics, are also sensitive to the state of the materials under study. While there is no doubt that the nuclear approach is highly developed and has been very successful, we believe that, in many cases, an equally strong program can be developed without the use of nuclear devices. The scale of NIF and other "superlasers," in terms of sample size and time scale, considered together with the highly developed diagnostic tools developed for the ICF effort world-wide, make credible a laboratory-scale effort.

As an example, we illustrate in Fig. 1a the experimental equation of state (EOS) of aluminum by showing its shock Hugoniot, that is, the pressure-density curve for shocked Al.(8) For pressures less than a few Mbar, the data were taken using high explosives or gas guns to accelerate flier

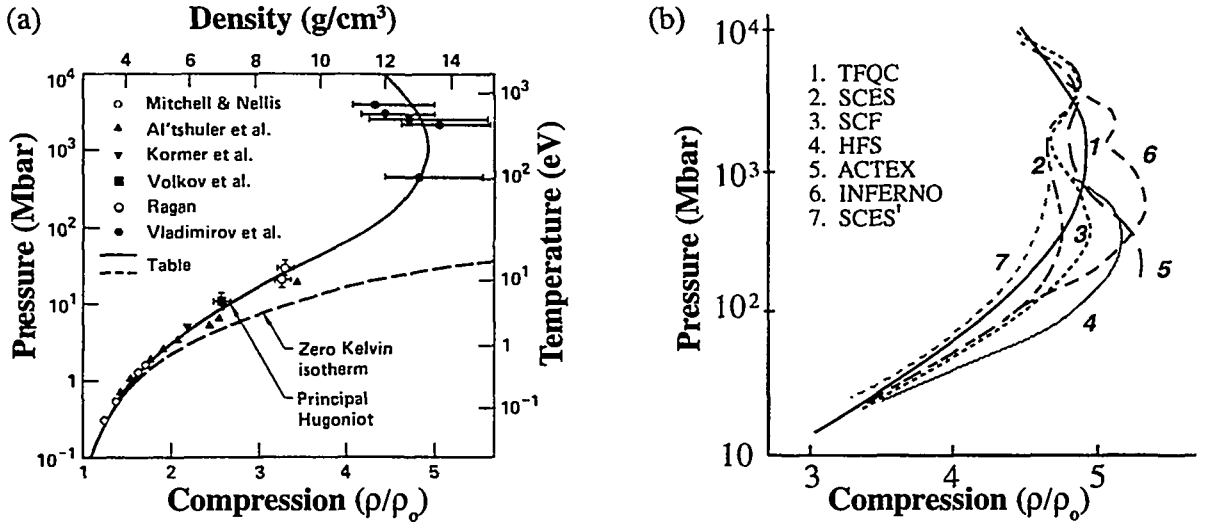

FIGURE 1. (a) A comparison (reproduced from Ref. 8) of experimental and tabular theoretical shock hugoniots for Al. Temperatures calculated from the table are indicated on the right vertical axis, and the 0 K isotherm is also shown for comparison. (b) Calculations of the principal Hugoniot of aluminum using a variety of theoretical methods (reproduced from Ref. 9). The pressure is expressed in Mbar.

plates. Pressures above a few Mbar correspond to data which were taken during underground nuclear detonations. Tables have been constructed to smoothly interpolate between the points, as shown by the solid curve in Fig. 1a.

The theoretical EOS for Al is illustrated in Fig. 1b.(9) The simplest and perhaps most widely used of the models is the statistical Thomas-Fermi model with quantum corrections (TFQC). This model does not include atomic shell structure, but rather treats the electron states as a continuum. The self-consistent field (SCF), Hartree-Fock-Slater (HFS), and INFERNO models treat the electron shells quantum mechanically, but differ in their handling of close-packed levels corresponding to energy bands. The semiclassical equation of state (SCES) model treats both the discrete electron shells and the energy bands semiclassically. The ACTEX model is an ionization equilibrium plasma model which uses effective electron-ion potentials fitted to experimental spectroscopic data. These models typically include the nuclear component using the ideal gas approximation. An exception is a Monte Carlo treatment of the thermal motion of the nuclei implemented in one of the version of the semiclassical equation of state (SCES'). The oscillations in the pressure versus compression curves shown in Fig. 1b result from the ionization of the K- and L-shell electrons of Al.

One is struck by the lack of convergence of the models in the pressure range of 50-1000 Mbar, namely, where the electron shell effects become important. The greatest variation in the models occurs around a pressure of 100 Mbar. The existing data in this region is too sparse and lacks sufficient accuracy to differentiate between the models. However, recent flier-plate experiments on the Nova laser achieved pressures of 750 Mbar,(10) highlighting the potential of using large lasers to fill in the experimental EOS curves in the critical range of 10-1000 Mbar.

The main difficulty in EOS experiments is determining the principle Hugoniot of materials (pressure versus density curve after single-shock compression) absolutely by simultaneous measurements of mass and shock velocities. The shock velocity is typically measured by recording the shock breakout times across known steps of a reference material. Determining the mass velocity is much more difficult. It has been measured successfully in nuclear driven experiments using gamma-reference layers(11) and neutron resonance Doppler shifts.(12) The gamma technique correponds to implanting into the material under study thin planar layers of, say, europium, which has a large

(n,γ) neutron capture cross section. During nuclear detonation, large neutron fluxes are produced, which, after being moderated to thermal energies, turn the reference layer into a strong gamma source. On the assumption that the reference layer flows with the bulk flow, one can view the γ-ray emission through colimated viewing slits from the side to deduce the mass velocity. The neutron resonance technique differs in that the mass velocity is determined by measuring the Doppler shifts of low-energy neutron resonances in the material behind the shock. In the case of lasers, the method of side-lighting a moving layer by x-rays is well established; efforts are underway to improve its level of accuracy. For many metals at these pressures, the temperature is even more uncertain than the density. Using tracer dopants, it appears that simultaneous opacity experiments to characterize the temperature may be possible. Note that at extremely high pressures, the material behind the shock front will be highly ionized, and will become a strong source of x-rays. Radiative preheat of the material ahead of the shock front could become a significant effect.(8,13)

We often want to test materials off the principal Hugoniot, for example, on the isentropic release from shocked states, or on isochoric paths from normal densities. This can be performed in a variety of ways using the NIF, whose scale will make accurate measurements possible.(6) For example, shock and release into low-density foams,(14) or multiple shock compression of highly porous materials(15) offer complementary approaches toward achieving the desired states of matter. Most planetary or astrophysical applications lie on isentropic compression paths.(16) This is an area which has been studied mostly with static compression in diamond-anvil cells, which reach pressures up to ~0.3 TPa.(17) Above this pressure, laser experiments will be most useful, which is an area we wish to emphasize as a frontier of high pressure physics. And this is the area in which the NIF should excel, since most of the laser and diagnostics development has been aimed at generating and characterizing such states. .

Large lasers have been driven largely by the international ICF effort, and their application to other areas of fundamental research has yet to be explored fully. For example, electrical and thermal conductivities are unknown in this region, as are magnetic properties, although maintaining sufficiently low temperatures on laser experiments will be a great challenge. Likewise, the details of material structure at these conditions are unknown. It seems likely that new phase transitions may be found, not only as a result of pressure, but also due to high magnetic fields.

HYDRODYNAMIC MIXING

Hydrodynamic material mixing results primarily from three instabilities: the gravity driven Rayleigh-Taylor instability, its shock analog the Richtmyer-Meshkov instability, and the shear-driven Kelvin-Helmholtz instability. The typical situation for the Rayleigh-Taylor instability occurs at an interface between a low density (ρ_2) fluid and a high density (ρ_1) fluid. If the lighter fluid is accelerating the heavier fluid, then in the frame of reference of the interface, one effectively has a heavy fluid "sitting on top of" a light fluid. The interface is hydrodynamically unstable, and spatial perturbations η_o will grow exponentially in time, $\eta(t)=\eta_o e^{\gamma t}$. Classically the growth rate in linear regime is given by $\gamma = (Akg)^{1/2}$, with $A=(\rho_1-\rho_2)/(\rho_1+\rho_2)$ being the Atwood number, and $k=2\pi/\lambda$ being the perturbation wave number. In the nonlinear asymptotic limit, the interface evolves into bubbles of the lighter fluid rising at their terminal velocity of $v_B=0.3(g\lambda)^{1/2}$ (for A=1), and spikes of the heavier fluid falling through the lighter fluid.

A convenient categorization of the flow is given by the dimensionless Reynolds number, $R=Lu/\nu$, where L is the system size, u the characteristic fluid velocity, and ν the kinematic viscosity. Situations of high R ($> 10^3$) are prone to turbulent hydrodynamic mixing. This is easy to see. Large spatial size L means a large number of modes could grow; low viscosity ν means a broad range of modes do grow; and high fluid velocity u hastens the transition to turbulence through strong Kelvin-Helmholtz driven vorticity generation. The situation in a plasma is similar except for compression and ionization. Compression introduces an additional scale to the problem, namely, the density gradient scale length, and ionization causes the viscosity to drop to very low values. Hence plasmas can be extremely hydrodynamically unstable. Despite their small spatial scales, laser produced plasmas can have Reynolds numbers easily in excess of 10^6.

From situations as commonplace as the turbu-

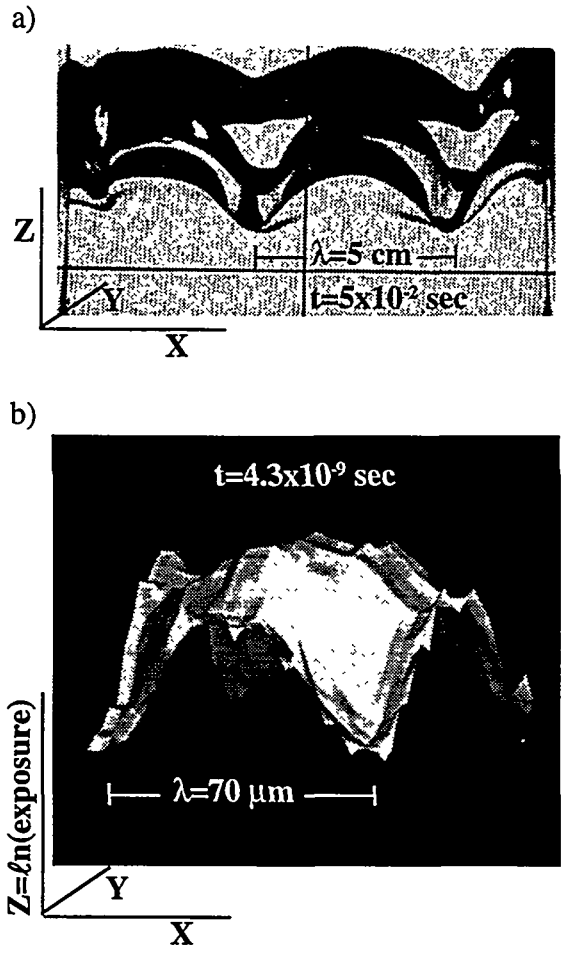

FIGURE 2. Comparison of three-dimensional $k_x=k_y$ single-mode Rayleigh-Taylor data taken (a) on a 12 cm, $5g_o$ macroscopic water-cell accelerator (reproduced from Ref. 19) and (b) on a 500 μm, $10^{13}g_o$ accelerated foil at the Nova laser (Ref. 20).

lent mixing of gasoline with air in the carburetor of one's car, to the violent core-envelope mixing that leads to the cataclysmic stellar explosions of supernovae,(18) nature is replete with examples of nonlinear hydrodynamic mixing. However, the area of turbulent hydrodynamics and material mixing remains one of the most theoretically intractable problems around. Experimental facilities in relevant regimes are essential to various modeling techniques.

One long-used method of investigating shock-induced compressible mixing due to the Richtmyer-Meshkov instability is the use of shock tubes. Here, the acceleration is impulsive, the pressures are typically only a few bar, the compression is low, the amount of perturbation growth is modest (growth factors of a few), and there is no radiation or ionization involved. High explosives generate pressures up to 200-300 kbar, but compression is low, there is no ionization or radiation, and diagnostic access is limited. Gas guns can generate pressures up to 1 Mbar, large perturbation growth, but with modest compression, diagnosis is difficult, and there is little radiation or ionization.(14) Macroscopic fluid-cell accelerators(19) deal with incompressible hydrodynamics at modest accelerations ($5\text{-}500g_o$). Perturbation growth factors can be large, diagnosis can be good, but there is no radiation, ionization, or compression involved. On large lasers like Nova and the NIF, the accelerations are extreme ($10^{13}\text{-}10^{14}g_o$), pressures of 100's of Mbar are routine, and one can achieve high growth factors, large compression, and high levels of radiation flow and ionization.(20) The situation in a nuclear detonation is similar, only all of the scales are larger.

The issue of macroscopic (say, as in nuclear testing) vs. microscopic (such as Nova or NIF) experiments needs to be addressed. As an example, we show in Fig. 2a data taken by Jacobs and Catton from a macroscopic (12 cm) water cell experiment(19) and in Fig. 2b results from Marinak *et al.* from a microscopic (500 μm) Nova experiment(20), both looking at the three-dimensional Rayleigh-Taylor evolution of a square $k_x=k_y$ surface perturbation. The water experiment was done with a pressure of about 0.1 bar, accelerating a 2 liter square water cell at $5g_o$ with no compression or radiation, and was diagnosed by side-on optical shadowgraphy. The Nova experiment was done at a pressure of 30 Mbar accelerating an initially 50 μm thick CH(Br) foil at $7x10^{12}g_o$ under high compression (5 times solid), with high levels of radiation flow, and diagnosed by face-on x-ray backlighting The microscopic imaging capabilities on Nova are indeed impressive,(21) with as much detail observable in the Nova experiment as in the macroscopic water experiment. Note that in comparing these two experiments, the spatial scales differ by 3 orders of magnitude, the time scales by 7 orders of magnitude, the pressures by over 8 orders of magnitude, and the accelerations differ by 12 orders of magnitude!

Figure 2 presents an excellent opportunity to com-

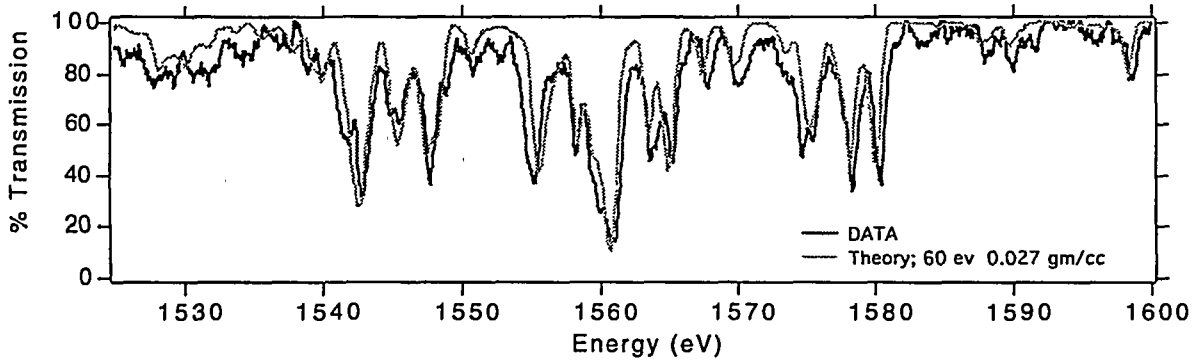

FIGURE 3. Nova experimental data for the LTE opacity of aluminum (from Ref. 26) compared to the OPAL code.

pare similar hydrodynamics in regimes of vastly different scale. To write down a scale transformation, we do the following. In the nonlinear regime, the fluid flow can be characterized by a spatial scale of order the perturbation wavelength λ and velocity of order the perturbation terminal bubble velocity $v_B=0.3(g\lambda)^{1/2}$. Hence, a characteristic time is given by $\tau=\lambda/v_B=(\lambda/g)^{1/2}$, dropping factors of 2. One gets the same result in the linear regime by writing the characteristic time as $\tau=1/\gamma=1/(kg)^{1/2}=(\lambda/g)^{1/2}$, again dropping factors of 2. Hence, the scale transformation taking λ to $a_1\lambda$ and g to a_2g requires that τ goes to $(a_1/a_2)^{1/2}\tau$ for the hydrodynamic equations to be invariant.

Based on the similar shapes of the perturbations shown in Figs. 2a and 2b, these two experiments appear to be accessing the same nonlinear hydrodynamics, so we can test this scale transformation. The scale factors relating spatial scale and acceleration are given by $a_1=\lambda_{micro}/\lambda_{macro}=1.4\text{x}10^{-3}$, and $a_2=g_{micro}/g_{macro}=1.4\text{x}10^{12}$, where the subscripts "micro" and "macro" refer to the laser and water cell experiments, respectively. The corresponding scaled time is then given by $\tau=(a_1/a_2)^{1/2}(5\text{x}10^{-2}\text{sec})=1.6\text{x}10^{-9}\text{sec}$. This compares well with the actual $\tau_{RT}=4.3\text{-}2.5=1.8$ ns of the laser experiment in Fig. 2b, which represents the duration of foil acceleration after shock breakout which occurs at 2.5 ns. Scale transformations of the hydrodynamics equations are straight forward, and one can learn much from simple experiments on incompressible fluids. A quantitative understanding of hydrodynamic mixing relevant to ICF and nuclear applications, however, requires experiments done at high compression with radiation flow. Rapid material compression leads to the launching of strong shocks, which contribute to the mixing through the Richtmyer-Meshkov instability. And radiation flow leads to density gradients and to mass ablation, both of which affect the degree of mixing.

RADIATION PHYSICS

The study of radiation physics is a central part of high energy density research. Almost by definition, "high energy density physics," denotes a regime wherethe emission and absorption of radiation (usually x-rays) from stripped ions, and the transport of that radiation forms an important part of the energy balance of the medium.

The study of radiation physics can be described in three somewhat interwoven categories. The first is the study of the radiative properties of stripped atoms in plasmas, which ranges from the study of the atomic spectroscopy of isolated ions, to the study of complex radiation opacities.(22) The latter involves consideration of an enormous number of relevant ionic states and transitions (up to 10^8 in the case of M-band dominated opacities) and the effects of plasma on them (23). The second category involves the application of such radiative properties to situations such as the behavior of an inertial confinement fusion hohlraum (radiation cavity), or the significant role of new metal opacity theory in models of pulsating stars such as Cepheid variables (24). Finally, the third category is the practical application of radiation physics to the development of new techniques for plasma diagnostics and potentially for other fields such as medical physics (25).

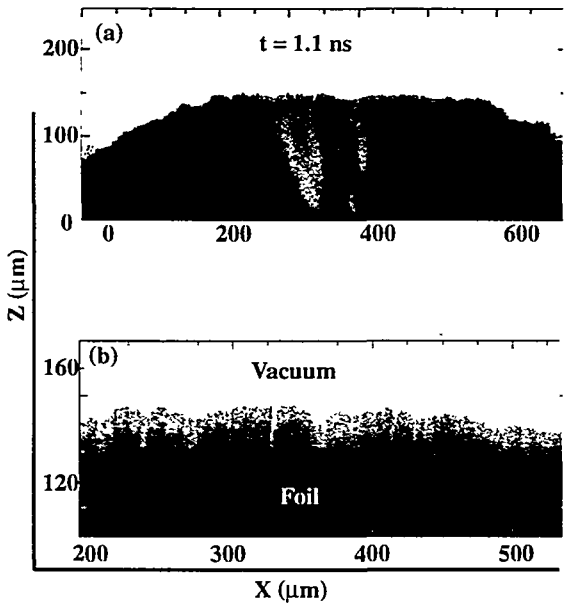

FIGURE 4. (a) Side-on x-ray laser radiograph taken at 30x magnification at time 1.1 ns of a foil accelerated by a 1 ns Nova pulse at wavelength λ_{Laser}=528 nm and intensity I=10^{14}W/cm^2. The foil consisted of a 10 μm CH ablator backed by a 3 μm Al payload. The laser was incident on the CH ablator from below, generating an ablation pressure of ~20 Mbar, which accelerated the foil at $10^{13}g_o$, where g_o is the acceleration due to gravity. The foil was originally located at zero on the vertical scale. (b) Enlarged view of the central portion of (a) showing 5 μm structures. (This figure was reproduced from Ref. 28.)

As an example of the "second category," experiments done at the Nova laser have already demonstrated (26) the ability to prepare a uniform, x-ray heated sample in local thermodynamic equilibrium (LTE), and to measure its opacity through a point projection spectroscopic method. Figure 3 shows the results for such a transmission spectrum for aluminum at about 60 eV compared to calculations using the modern detailed accounting code OPAL (24). This method was also used to verify the OPAL predictions for Fe opacities at astrophysically interesting x-ray energies (26). The code result and its experimental verification turned out to be so precise that the code can now be used as a thermometer that is accurate to a few percent for use in other experiments

An example from our "third category" of the feedback of laser physics experiments into a useful diagnostic lies in the non-LTE plasma experiments that led to the discovery and development of x-ray lasers at Nova and other large lasers (27). In figure 4 we show how the x-ray laser's extraordinary effective brightness (10^{17}W/cm^2-Å-ster, which is the equivalent of a 6 Gev black body) is being used to image the column densities of hot dense plasmas down to the micron scale with 50 ps time resolution (28). The x-ray laser is also being explored as a potential tool for use in the medical field for precise imaging of microscopic biological specimens.(25) From these examples of work done at Nova (operating from ~1 to 50 kilojoules) and other lasers, we may infer that the megajoule class lasers will allow us to extend the study of radiative properties of LTE and non-LTE matter to far higher Z, densities, and temperatures, and to use these new radiative sources as diagnostics.

SUMMARY

Nuclear experiments offer the unique possibility of bringing very large volumes of material into high energy density conditions, and experiments that require that feature are likely to remain solely in the province of nuclear experimentation. However, such experiments are expensive, and are difficult to diagnose with high precision. In contrast, the megajoule-class superlasers such as the NIF will be able to conduct experimental campaigns at a shot rate of over 4 shots per day. Therefore, the laser experiments offer the possibility of extensive parameter variation, control, and diagnostic development. Examples of this ability to control the experiments are: the ubiquitous use of timed x-ray backlighters to "photograph" the hydrodynamic instability of the sort shown in Fig. 2b, or to measure the transmission spectrum of the LTE opacity sample shown in Fig. 3. Another less obvious advantage of the laser based experiments is the ease of preparing samples that are optically thin and are thus fully diagnosable. For example, analysis of hydrodynamic instabilities such as that shown in Fig. 2b require in general a three dimensional reconstruction of the target. This is only possible for samples that are optically thin to the relevant backlighter.

ACKNOWLEDGMENTS

This work was performed under the auspices of the U.S. Department of Energy by the Lawrence Livermore National Laboratory under contract No. W-

7405-ENG-48.

REFERENCES

1. E. N. Avrorin, B.V. Litvinov, and V.A. Simonenko, proposal, "Uses of Nuclear Explosivions for Fundamental Research", in preparation (1995).
2. J.A. Paisner, E.M. Campbell, and W.J. Hogan, Fusion Technology **26**, 755 (1994).
3. CHOCS No. 13, Avril 1995, Revue Scientifique et Technique de la Direction des Applications Militaires, CEA; M. Andre, "Conceptual Design of the French LMJ Laser," First Annual International Conference on Solid State Lasers for Application to ICF, Monterey, CA, May 31 – June 1 (1995), SPIE proceedings.
4. J. Nuckolls *et al.*, Nature **239**, 139 (1972).
5. J. D. Lindl and W. C. Mead, Phys. Rev. Lett. **34**, 1273 (1975).
6. R. W. Lee *et al.*, "Science on High Energy Lasers From Today to the NIF," UCRL-ID-119170.
7. E.N. Avrorin *et al.*, Physics-Uspekhi **36**, 337 (1993).
8. D.A. Young *et al.*, Phys. Lett. **108A**, 157 (1985).
9. E. Avrorin *et al.*, Sov. Physics JETP **66**, 348 (1987).
10. R. W. Cauble *et al.*, Phys. Rev. Lett. **70**, 2102 (1993).
11. V.A. Simonenko *et al.*, Sov. Phys. JETP **61**, 869 (1985).
12. C. E. Ragan III, M. G. Silbert, and B. C. Diven, J. Appl. Phys. **48**, 2860 (1977).
13. Ya. B. Zel'dovich and Yu. P. Raizer, *Physics of Shock Waves and High-Temperature Hydrodynamic Phenomena*, (Academic Press, New York, 1967).
14. N.C. Holmes *et al.*, Appl. Phys. Lett **45**, 626(1984); N. C. Holmes, in *High-Pressure Sceince and Technology–1993*, ed. by S.C. Schmidt *et al.*, (AIP, New York, 1991), p. 153.
15. Ya. B. Zel'dovich, Sov. Phys. JETP **5**,1103 (1957).; N.C. Holmes, Rev. Sci. Instrum. **62**,1990(1991); I. V. Lomonosov, A. V. Bushman, and V. E. Fortov, in *High-Pressure Sceince and Technology–1993*, ed. by S.C. Schmidt *et al.*, (AIP, New York, 1991), p. 117–124.
16. W. B. Hubbard and R. Smoluchowski, Space Science Reviews **14**, 599 (1973); D. J. Stevenson, Annual Reviews of Earth and Planetary Sciences **10**, 257 (1982).
17. J. Akella, in *High Pressure Science and Technology – 1993*, ed. by S.C. Schmidt *et al.* (AIP, New York, 1993), p.187.
18. E. Muller, B. Fryxell, and D. Arnett, Astron. Astrophys. **251**, 505 (1991).
19. Jacobs and Catton, J. Fluid Mech. **187**, 353 (1988).
20. Marinak *et al.*, Phys. Rev. Lett., in press (1995); B.A. Remington *et al.*, Phys. Plasmas **2**, 241 (1995).
21. J.D. Kilkenny, Rev. Sci. Instrum. **63**, 4688 (1992).
22. D.R. Inglis and E. Teller, Ap. J. **90**, 439 (1939); M. Goeppert Mayer, Phys. Rev. **60**, 184 (1941); C.E. Moore, NBS Circ. **467**, 1 (1949); W.J. Karzas and R. Latter, Ap. J.**134**, 665 (1961) and Ap. J. Suppl. **6**, 167 (1961); A.N. Cox and J.E. Tablr, Ap. J. Suppl. **31**, 271 (1976); and N.H. Magee Jr., A.L. Merts, and W.F. Huebner, Ap. J. **283**, 264 (1984).
23. A. Bar-Shalom, J. Oreg, W. H. Goldstein, D. Shvarts, and A. Zigler, Phys. Rev. A. **40**, 3183(1989).
24. F. J. Rogers and C. A. Iglesias, Science **263**,50(1994).
25. L. B. DaSilva *et al.*, Science **258**, 269 (1992).
26. T. S. Perry *et. al*, " Phys. Rev. Lett., **67**, 3784, (1991); L. Da Silva *et. al.*, Phys. Rev. Lett., **69**, 438, (1992); P. T. Springer *et. al.* Phys. Rev. Lett., **69**, 3735, (1992).
27. R. Elton, *X-Ray Lasers*, New York, Academic Press, 1990; D. C. Eder and D. L. Mathews, *X-ray Lasers 1994 – 4th International Collloquium*, (AIP Conference Proceedings **332**, 1994).
28. R. C. Cauble *et al.*, Phys. Rev. Lett. **74**, 3816 (1995).